Current Science
CS 5 (5), 4659-4677 (2025)
Received 13 June 2025 | **Revised 15 July** 2025 | **Accepted 20 August** 2025 | **Online Available 30 September** 2025
https://doi.org0/10.52845/CS/2025-5-5-25

Current Science

Current Science

OPEN ACCESS

ISSN(O)2795-8639

Research Article

Exploring the Altered Immune Microenvironment of Gastric Signet Ring Cell Carcinoma and Predicting Therapeutic Targets of Pseudobulbus Cremastrae Seu Pleiones using Single-Cell RNA Sequencing Combined with Network Pharmacology

Aoqiang Zhou[1], Zhen Chen[2], Haiqun Lin[3, 4], Leng Li[2]*

[1]State Key Laboratory of Dampness Syndrome of Chinese Medicine, The Second Affiliated Hospital of Guangzhou University of Chinese Medicine, Guangzhou 510120, Guangdong Province, China

[2]Respiratory department, Dongguan Hospital of Guangzhou University of Chinese Medicine, Dongguan 523000, Guangdong, China

[3]Department of Graduate School, Guangzhou University of Chinese Medicine, Guangzhou 510120, Guangdong, China

[4]The Master Degree Application of Equivalent Educational Level of Guangzhou University of Chinese Medicine, Guangzhou 510120, Guangdong, China

[*]Corresponding Author: Leng Li

Abstract:

Background: Macrophages serve as crucial mediators in the progression of gastric signet ring cell carcinoma (GSRCC), while Pseudobulbus Cremastrae seu Pleiones (PCsP), a traditional Chinese medicine, demonstrates efficacy in promoting apoptotic processes in cancer cells. Our aim is to elucidate macrophage heterogeneity within GSRCC tissues and to delineate the therapeutic mechanisms of PCsP in regulating tumor microenvironment (TME).

Methods: Transcriptional profiling of GSRCC specimens was performed to elucidate the macrophage-associated gene expression patterns for intercellular communication and trajectory analyses. The TCMSP and Swiss Target Prediction databases were used to identify bioactive constituents of PCsP and their corresponding molecular targets. The Metascape platform facilitated GO and KEGG pathway analyses, while molecular docking simulations were conducted to evaluate component-gene binding affinities.

Results: Tumor-associated macrophages (TAMs) exhibited significant higher proliferation rates compared to normal tissue counterparts. Further stratification of TAMs identified 7 distinct subtypes. Temporal trajectory analysis revealed three distinct developmental states and four discrete gene expression modules within the macrophage population. A subsequent analysis of the intercellular communication network revealed enhanced signalling interactions between the TME and other cells. Eight bioactive constituents of PCsP and 489 GSRCC-associated target genes were identified based on the databases. PPI network analysis indicated 8 highest-centrality targets of PCsP. KEGG pathway analysis suggested predominant roles for lipid and atherosclerosis signaling pathways in GSRCC suppression. Molecular docking studies confirmed robust binding affinities between PCsP's primary constituents and central genetic targets.

Conclusions: This investigation identified alterations of TME in GSRCC, proposes a hypothesis for a potential mechanism of PCsP.

Keywords: Gastric signet ring cell carcinoma; tumor-associated macrophages; single-cell RNA sequencing; network pharmacological analyses; traditional Chinese medicine.

1. Introduction

Gastric cancer (GC) ranks as the fifth most commonly diagnosed malignancies and fourth leading cause of cancer-related mortality worldwide[1-3]. Gastric signet ring cell carcinoma (GSRCC), a distinct entity within the diffuse-type of GC, characterized by unique morphological features and aggressive clinical prognosis that poses therapeutic challenges [4, 5]. Surgery followed by adjuvant chemotherapy or chemoradiotherapy is the standard-of-care treatment for half of GC patients [6, 7]. Recent therapeutic innovations have introduced precision medicine approaches, including immune checkpoint inhibitors (ICIs) [8, 9]. Despite these therapeutic advances, GSRCC patients continue to exhibit poor prognostic outcomes, with reported median survival durations consistently falling between 12 and 20 months according to recent clinical studies[10, 11]. As a complementary and alternative therapy, traditional Chinese medicine (TCM) has been playing a significant role in GC treatment. Some systematic reviews demonstrated the beneficial effects of TCM in improving survival, myelosuppression and immune function of GC patients[12]. However, significant knowledge gaps persist regarding the molecular mechanisms, active pharmaceutical ingredients and specific therapeutic targets of TCM in GSRCC.

The tumor microenvironment (TME) in GC manifests unique heterogeneous characteristics that have emerged as a focal point in oncological research[13-16]. The TME functions as a critical regulator of neoplastic progression, exercising profound influence over invasive capabilities, metastatic propensity, immune system circumvention, and therapeutic resilience[17]. Tumor-associated macrophages (TAMs) in the TME serve as fundamental constituents, exhibiting exceptional phenotypic adaptability in response to microenvironmental cues[18]. A comprehensive elucidation of the molecular determinants governing macrophage phenotypic plasticity and functional dynamics within GC emerge as an imperative prerequisite for the development of efficacious immunotherapeutic interventions[19]. With the continuous development of sequencing technology, the single-cell RNA sequencing (scRNA-seq) methodologies has transformed our capability to conduct high-fidelity transcriptional analyses across heterogeneous cellular populations, encompassing both neoplastic and stromal components that modulate tumor progression and metastatic cascades[20].

The therapeutic implementation of TCM in oncological interventions has been extensively documented throughout multiple millennia. This medical paradigm exhibiting substantial efficacy in cancer immunotherapy[21]. Pseudobulbus Cremastrae seu Pleiones (PCsP), has multiple therapeutic applications, including antipyretic properties, detoxification, mucolytic functions, and cancer cell growth inhibition[22] . Recent pharmacological investigations have elucidated antineoplastic properties of PCsP manifested through multiple mechanisms including cellular proliferation inhibition, programmed cell death induction, and metastatic cascade suppression [23]. However, the precise molecular mechanisms underlying the antineoplastic efficacy and immue modulation of PCsP in GSRCC require further elucidation. The burgeoning domain of network pharmacology, which integrates systems biology paradigms with computational network analytics, illuminates the complex molecular orchestration between phytochemical constituents, genomic elements, and their corresponding cellular targets through the construction and analysis of intricate network topological architectures. Using network pharmacology and molecular docking method can be applied to elucidate the potential active ingredient and potential anti-cancer mechanism of PCsP.

In our study, our aim is to elucidate macrophage heterogeneity within GSRCC tissues utilizing single-cell RNA sequencing (scRNA-seq) methodology and to delineate the therapeutic mechanisms of PCsP in regulating TME especially through comprehensive network pharmacological analyses in GSRCC. The flow chart of studying the active ingredients of PCsP and its immune modulation in GSRCC using scRNA-seq and network pharmacology was showed in Figure 1.

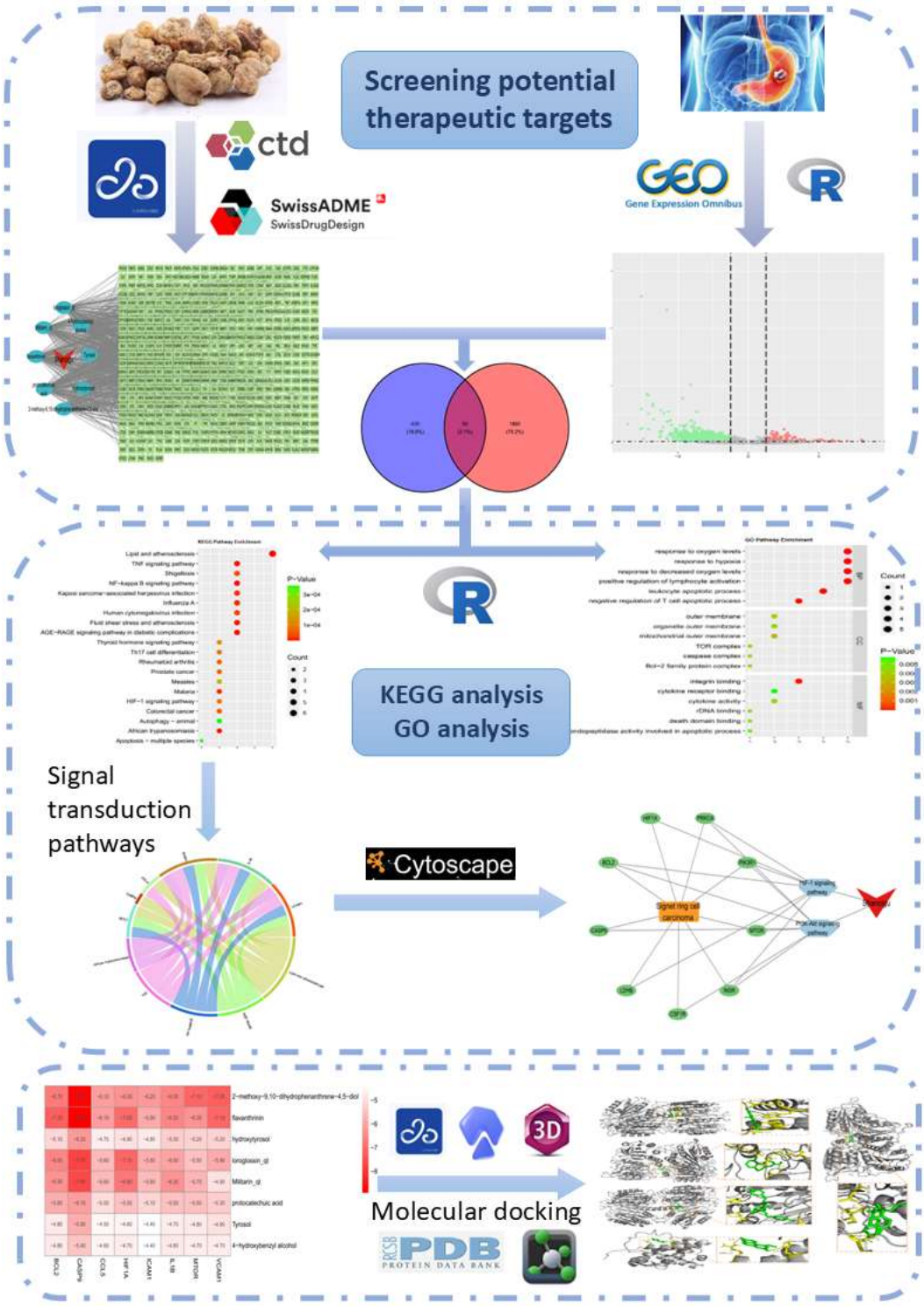

Figure 1 The flow chart of studying the active ingredients of PCsP and its immune modulation in GSRCC using scRNA-seq and network pharmacology

2 Materials and Methods

2.1 Data Acquisition and Processing

The transcriptomic profiles at single-cell resolution were acquired from the Gene Expression Omnibus repository (accession number GSE163558). The molecular data, including gene-barcode matrices, feature annotations, and unique molecular identifier (UMI) quantification tables, were previously documented in accordance with the protocols established by Jiang H and colleagues[24]. Given the public domain status of these datasets, institutional ethical review was deemed unnecessary. Quality filtration parameters were implemented to ensure data integrity: cells

expressing fewer than 250 genes were excluded, genes were required to demonstrate expression in a minimum of three cells, and specimens exhibiting mitochondrial transcript proportions exceeding 20% were eliminated.

2.2 Dimensionality Reduction and Cellular Clustering

The quality-filtered expression matrices underwent normalization through the implementation of Seurat's Normalize Data algorithm. Subsequently, the Find Variable Features computational method identified 2,000 genes exhibiting significant variability, which were then subjected to standardization utilizing the Scale Data functionality. The primary cellular populations were distinguished using a clustering resolution parameter of 0.7, whereas sub-clustering analyses employed a 0.6 resolution parameter to elucidate sample-specific cellular composition variations. The final visualization framework utilized the Uniform Manifold Approximation and Projection algorithm, executed through Run UMAP with dimensional parameters spanning 1:30.

2.3 Marker Gene Analysis and Cell-Type Annotation

The identification of differential marker genes across cellular populations was executed through implementation of the Seurat Find Markers algorithm, employing bimodal likelihood ratio assessment protocols. Cellular cluster annotations were derived through systematic evaluation of well-characterized canonical markers and their documented functional attributes in peer-reviewed literature. Expression patterns specific to individual cell populations were visualized through the generation of comprehensive heatmaps, dot plots, and violin plots utilizing specialized Seurat visualization modules.

2.4 Differentially Expressed Gene Analysis

The characterization of differentially expressed genes (DEGs) within cellular clusters was accomplished utilizing the Seurat Find Markers computational framework. Statistical evaluation of gene expression heterogeneity between cellular subpopulations was conducted through implementation of the Wilcoxon rank-sum test with integrated Bonferroni adjustment.

2.5 Pseudotemporal Trajectory Analysis

The investigation of transcriptional dynamics and cellular state transitions across primary clusters and their subpopulations was performed through pseudotemporal progression analysis employing the Monocle2 R package (version 2.14.0). Temporal expression patterns were subsequently visualized through a representative heatmap generated via the plot Pseudotime Heatmap functionality. The establishment of four distinct modulatory clusters was achieved by configuring the numcluster parameter appropriately, facilitating the identification of gene cohorts exhibiting coordinated temporal expression trajectories.

2.6 Intercellular Communication Analysis

The reconstruction of intercellular signaling networks was accomplished through comprehensive analysis of ligand-receptor interaction profiles utilizing the Cell Chat DB analytical framework within the Cell Chat package. The core analytical workflow encompassed the sequential implementation of compute Commun Prob Pathway, compute Commun Prob, and aggregate Net functions. The assessment of differential interaction patterns between experimental cohorts was conducted utilizing a statistical significance threshold criterion of $p < 0.05$.

2.7 Compound Analysis and Target Identification Protocol

A comprehensive phytochemical investigation of PCSP constituents was conducted utilizing the Traditional Chinese Medicine Systems Pharmacology (TCMSP) database. Bioactive compounds were filtered based on predetermined pharmacokinetic parameters: oral bioavailability exceeding 30% and drug-likeness indices surpassing 0.18. The molecular targets were elucidated through the Swiss Target Prediction platform, followed by mining the Comparative Toxicogenomics Database to identify genetic elements specifically implicated in gastric cancer pathogenesis, with particular emphasis on signet ring cell carcinoma.

2.8 Intersection Analysis of Therapeutic and Disease Targets

The molecular interface between PCsP's pharmacologically active constituents and GSRCC pathophysiology was delineated through comparative analysis utilizing the Venny 2.1

platform.

2.9 Network Analysis of Drug-Compound-Target-Disease Interactions

A comprehensive network analysis was conducted utilizing the Cytoscape 3.9.1 platform to delineate the intricate relationships between PCsP's bioactive constituents and GSRCC. The network topology comprised nodes representing the convergent target genes between PCsP's bioactive constituents and GSRCC-associated genes, with interconnecting edges illustrating their functional associations.

2.10 Analysis of Protein-Protein Interaction Networks

The identified target genes were subjected to protein-protein interaction analysis via the STRING database, specifically parameterized for Homo sapiens proteome analysis. Subsequently, the derived interaction network underwent systematic topological analysis utilizing Cytoscape 3.7.1. Module identification within the resultant PPI network was executed through the MCODE algorithm, employing the following parametric constraints: Degree Cutoff: 2, K-core: 2, Node Score Cutoff: 0.2, and Maximum Depth: 100.

2.11 Gene Ontology and Pathway Enrichment Analysis

Intersection target-associated genes underwent comprehensive analysis utilizing the DAVID bioinformatics platform (accessed December 15, 2024). The analysis encompassed Gene Ontology (GO) term enrichment and Kyoto Encyclopedia of Genes and Genomes (KEGG) pathway mapping.

2.12 Network Construction

A comprehensive herb-compound-target interactome was established and rendered using Cytoscape to elucidate the mechanistic relationships between biochemical constituents and their molecular targets.

2.13 Compound-Target-Pathway Network

Cytoscape-based network analysis was implemented to construct and examine multidimensional interactions among bioactive compounds, molecular targets, and signaling pathways.

2.14 Molecular Docking

Computational ligand-receptor interaction analysis was performed to investigate binding characteristics between PCsP's bioactive constituents and identified hub genes. High-resolution crystallographic structures were acquired from the RCSB Protein Data Bank (accessed December 25, 2024). Three-dimensional molecular structures of PCsP constituents were obtained from PubChem (accessed December 28, 2024).

Receptor preparation was executed using Py MOL 2.6.0a0, incorporating the removal of crystallographic water molecules and co-crystallized ligands. Auto Dock Tools 4.2 (accessed January 2, 2025) facilitated the prediction of optimal binding conformations, with binding energy thresholds set at -5 kcal/mol or lower indicating favorable interactions.

3 Results

3.1 Single-cell Transcriptomic Analysis of Gastric Cancer and Adjacent Normal Tissues

Comprehensive examination of the GSE163558 single-cell RNA sequencing dataset, revealed 15,138 cells meeting rigorous quality parameters. Implementation of Uniform Manifold Approximation and Projection (UMAP) dimensionality reduction techniques facilitated the identification of 18 discrete cellular populations. Through the systematic integration of our single-cell transcriptomic profiles with established scientific literature, we delineated eight principal immune cell subsets within the GSRCC microenvironment. UMAP-based visualization demonstrated preserved clustering architectures across both neoplastic and non-neoplastic specimens when evaluated against the consolidated analysis.Quantitative analysis of cellular distributions necessitated normalization to account for differential cellular densities between neoplastic and non-neoplastic specimens, with results expressed as proportional representations. Most notably, there was a marked expansion of the macrophage population, which exhibited an 18.7-fold enrichment in neoplastic tissue (27.64%) compared to non-neoplastic tissue (1.48%) (Figure 2).

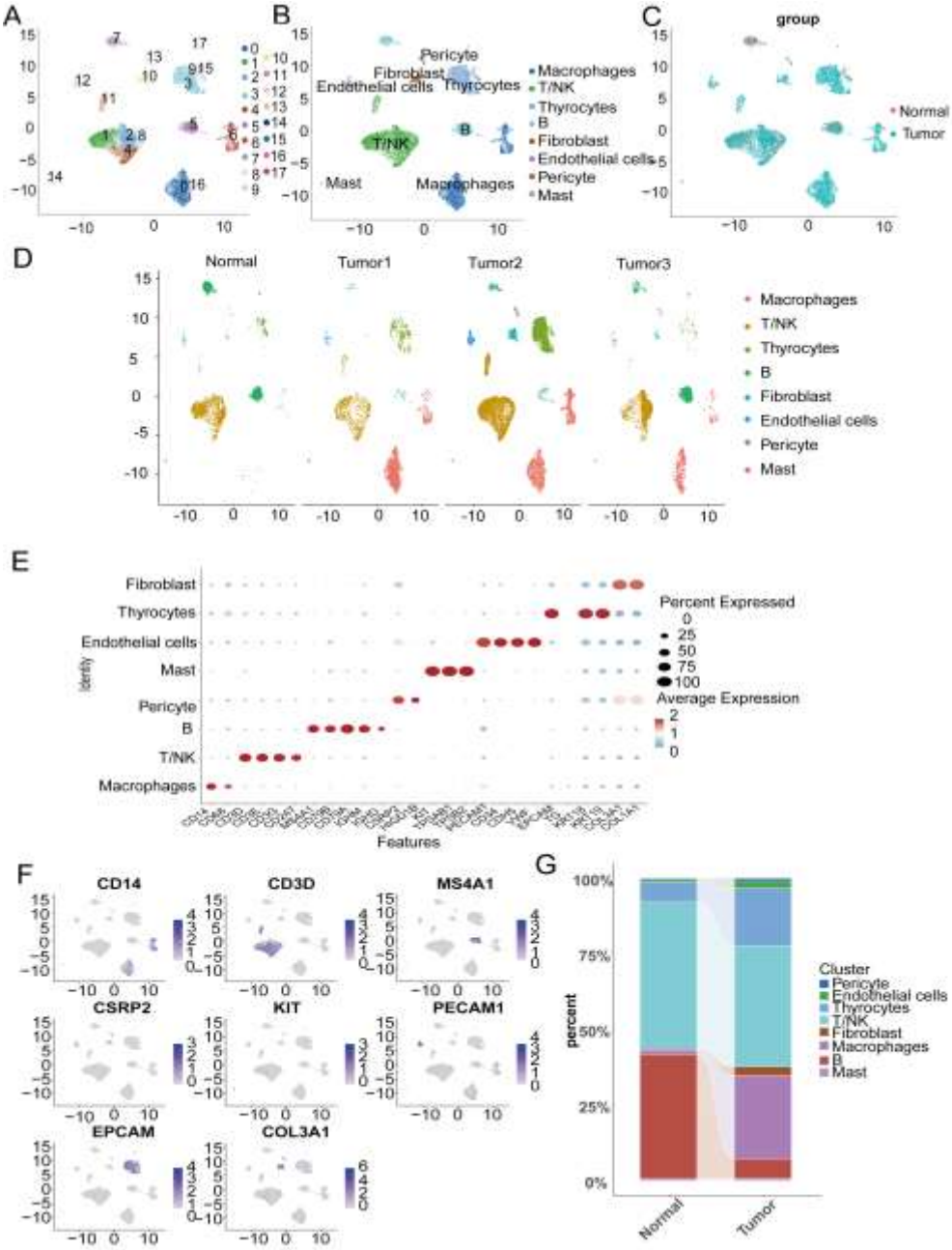

Figure 2 Single-cell atlas of gastric signet-ring cell carcinoma and normal samples. (A)UMAP plot colored by various cell clusters; (B)UMAP plot colored by subpopulation of cells after annotation; (C) UMAP plots of the gastric signet-ring cell carcinoma group (three samples) and normal group (one samples); (D)UMAP plots of different samples; (E) Dot plot of selected marker genes for each cell type; (F) Bar plot depicting the proportions of the eight main cell types in the gastric signet-ring cell carcinoma and normal groups; (G) Feature plots of selected marker genes for each cell type.

3.2 Single-Cell Transcriptomic Profiling and Functional Enrichment Analysis of Macrophage Populations via scRNA Seq

We subsequently extracted and conducted in-depth analyses on 3,582 macrophages to elucidate their phenotypic and functional characteristics. Unsupervised hierarchical clustering revealed seven distinct macrophage populations. Further molecular characterization facilitated the identification of seven discrete subsets, comprising 1,888 Mac1, 609 Mac2, 457 Mac3, 435 Mac4, 119 Mac5, 53 Mac6, and 21 Mac7 cells. Dimensionality reduction analysis utilizing Uniform Manifold Approximation and Projection (UMAP) illustrated comparable distribution patterns between neoplastic signet-ring cell specimens and their corresponding non-

transformed tissues, aligning with our initial comprehensive assessment. Through differential gene expression analyses, we identified subset-specific molecular signatures, characterized by the expression of TLR4, CD69, TNF, CD163, CD80, LOX, and IRF4. Furthermore, we delineated the seven most significantly upregulated genes that distinguished each macrophage subpopulation.The spatial distribution of cellular populations was evaluated through normalized proportional analysis to address variations in cellular density between neoplastic and control specimens. Quantitative examination demonstrated a significant upregulation of Mac1 subpopulations within neoplastic microenvironments, reaching 53.04% compared to the baseline level of 17.64% observed in non-transformed tissues. By contrast, Mac4 exhibited pronounced downregulation in malignant samples, with representation declining to 11.92% from 35.29% in healthy tissue controls (Figure 3).

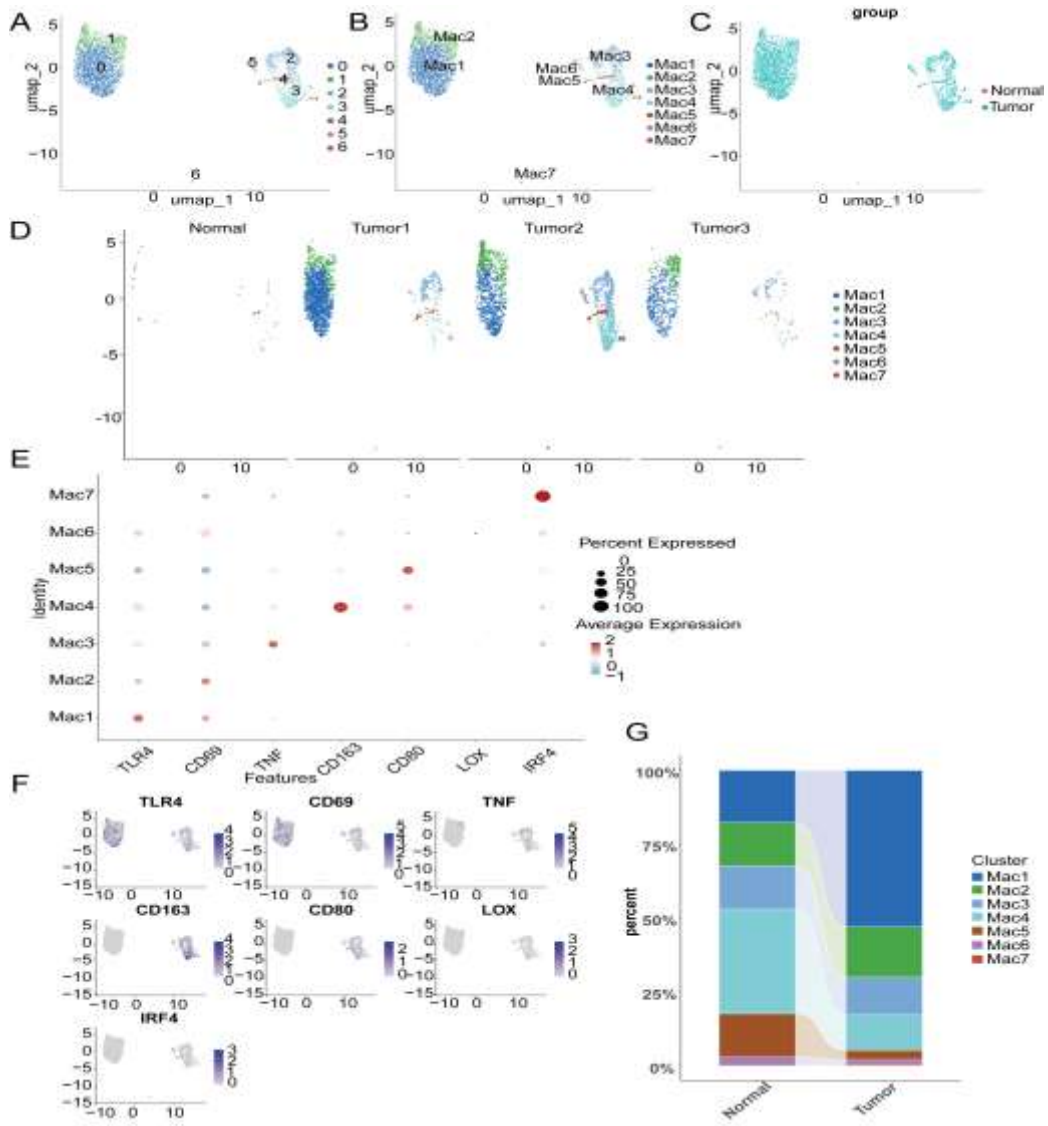

Figure 3 Alterations in macrophage cell subtypes during gastric signet-ring cell carcinoma. (A) UMAP plot colored by various macrophage cell clusters; (B) UMAP plot colored by subpopulation of macrophage cells after annotation; (C) UMAP plots of the signet-ring cell carcinoma group (three samples) and normal group (one samples); (D) UMAP plots of different samples; (E) Dot plot of selected marker genes for each macrophage cell type; (F) Bar plot depicting the proportions of the seven main macrophage cell types in the gastric signet-ring cell carcinoma and normal groups; (G) Feature plots of selected marker genes for each macrophage cell type.

3.3 Simulation of the development trajectory of macrophages and the analysis of gene expression pattern

The temporal evolution and transcriptomic landscapes of distinct macrophage subpopulations were systematically characterized through comprehensive pseudotemporal analyses, thereby illuminating their mechanistic contributions to signet-ring cell carcinoma pathogenesis. Spatiotemporal mapping demonstrated distinctive topological distributions among the seven identified macrophage subsets. Longitudinal trajectory analysis revealed three discrete developmental states at key chronological transitions. The evolutionary progression was computationally reconstructed utilizing the Monocle2 algorithmic framework, with the initial state designated as the developmental origin. Longitudinal transcriptomic profiling along the pseudotemporal continuum unveiled four distinct gene expression modules, which were subjected to hierarchical clustering and visualized via heat map representation. The temporal expression dynamics of eight signature genes - CSF3R, CXCR2, FCGR3B, H3F3A, IFITM2, NAMPT, S100A8, and S100A9 - exhibited synchronized patterns across the identified macrophage states, providing robust validation of the hierarchical clustering outcomes demonstrated in the heat map analyses (Figure 4).

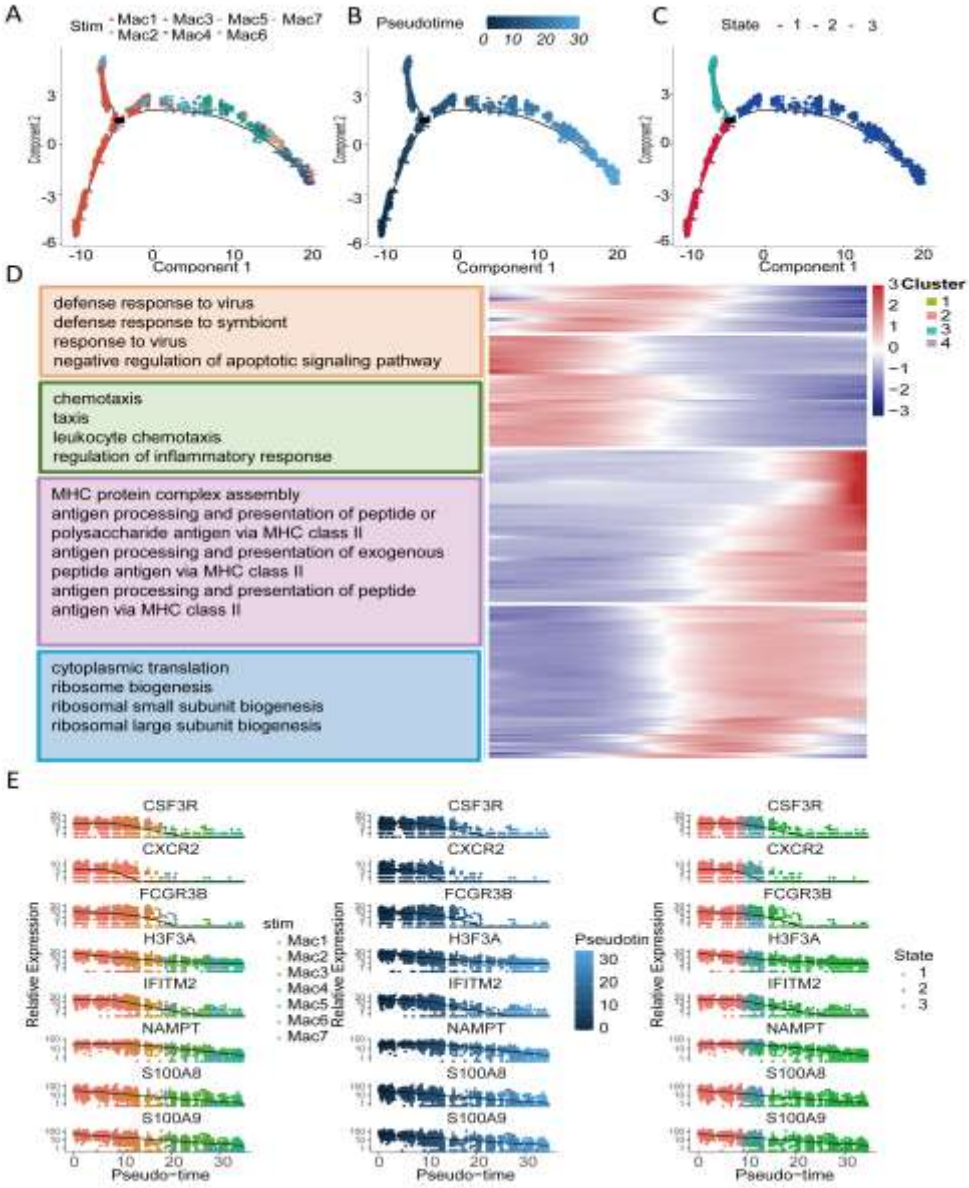

Figure 4 Simulation of the development trajectory of macrophage cells and the analysis of gene expression pattern inferred by Monocle2.
(A) Monocle. cell type; (B) Monocle. Pseudotime; (C) Monocle. State; (D) Heatmap _top; (E) Genes. monocle.

3.4 Cell-cell communication analysis

Analysis of intercellular communication networks revealed markedly elevated frequencies and intensities of cellular interactions within neoplastic tissues relative to normal tissue counterparts. The probabilistic assessment of heterotypic cellular interactions, delineates preferential communication patterns among discrete tumor cell populations, with notable reciprocal signaling observed between thyroid follicular cells and epithelial cellular constituents in the neoplastic milieu. Systematic evaluation of pathway dynamics uncovered distinctive alterations in both the distribution and robustness of intercellular signaling networks when comparing neoplastic versus physiological tissue specimens. This investigation identified substantial amplification of specific signaling cascades, particularly the VISFATIN, LAMININ, and MK pathways within neoplastic tissues, implicating their pivotal role in oncogenic progression. Moreover, granular examination of molecular interaction networks revealed marked perturbations in specific ligand-receptor engagement patterns within neoplastic tissues (Figure 5).

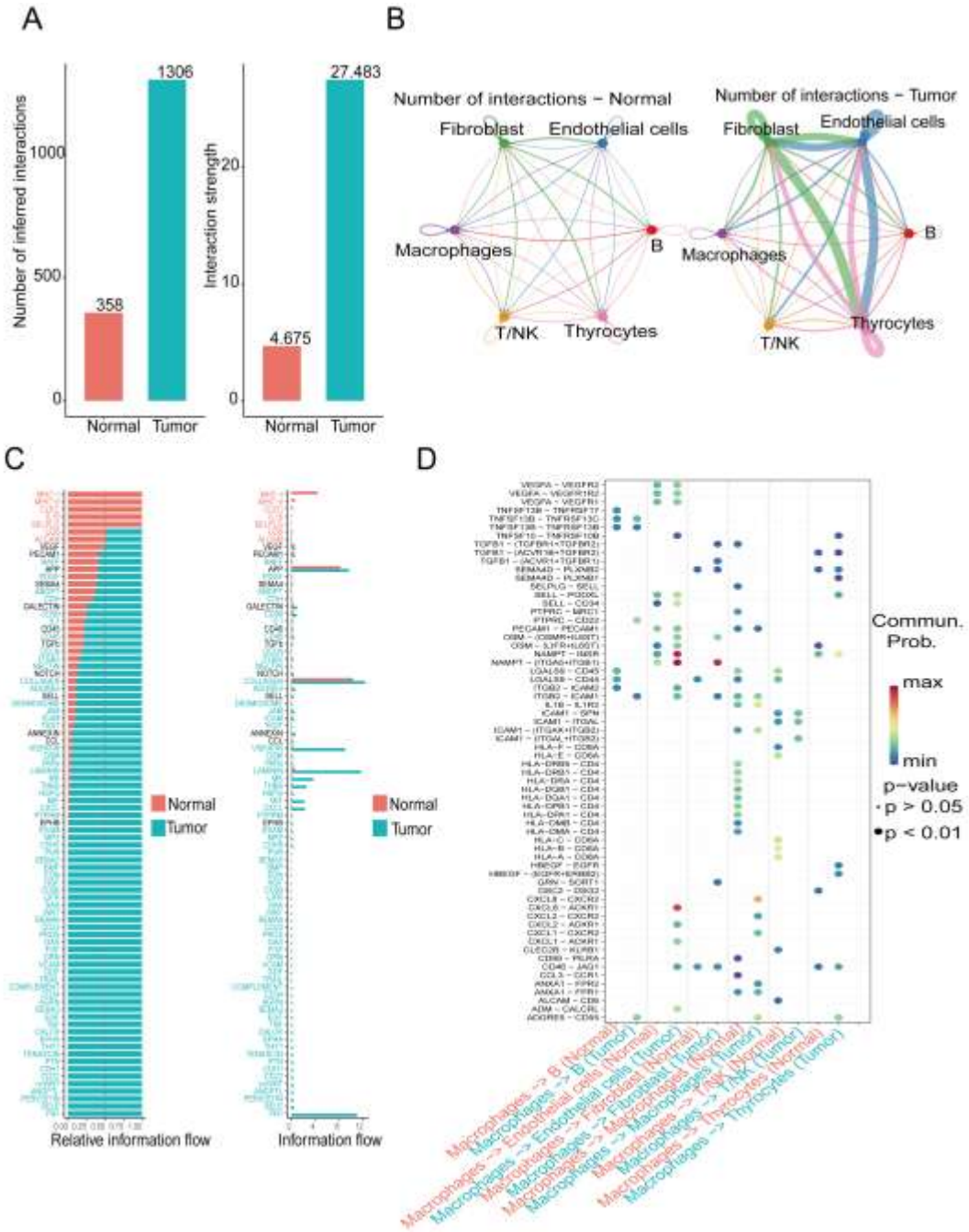

Figure 5 Communication network difference between the normal and gastric signet-ring cell

carcinoma tissue.
(A) Comparison of the number and intensity of cell communications between tumor and normal tissues;
(B) Interaction net count plot of non-tumor and tumor tissues;
(C) Differences in the number and intensity of signaling pathway-related cell communications between tumor and normal tissues;
(D) Key ligand-receptor pairs with significant changes in tumor and normal tissues.

3.5 Elucidation of Macrophage-Associated Targets and PCsP-Mediated Molecular Mechanisms in Gastric Carcinoma: An Integrated Pathway Analysis

A comprehensive bioinformatic investigation, employing multiple databases including the TCMSP, Swiss ADME, Comparative Toxicogenomics Database (CTD), and Swiss Target Prediction, facilitated the identification of eight bioactive constituents and 489 potential molecular targets associated with PCsP. Network pharmacological analyses were performed utilizing Cytoscape 3.7.2 to delineate the complex interactions between these bioactive components and their respective targets. This analysis culminated in the identification of 51 intersection targets warranting further investigation. Examination of the gene expression microarray dataset GSE163558, accessed through the Gene Expression Omnibus (GEO) repository, revealed significant transcriptional alterations in 1,968 genes, comprising 137 upregulated and 1,831 downregulated transcripts. These differential expression patterns are graphically represented in the volcano plot. To decipher the underlying biological mechanisms and signaling cascades modulated by PCsP in neoplastic cells, functional enrichment analysis was conducted on the 51 intersection targets utilizing the cluster Pro filer R package. This comprehensive analysis yielded 18 statistically significant GO classifications and 20 significantly enriched KEGG pathways. The enrichment analysis demonstrated that cellular response to oxygen levels and lipid-atherosclerosis pathways emerged as the predominant regulatory mechanisms. The protein-protein interaction network analysis revealed five highly significant KEGG pathways. These encompassed the lipid and atherosclerosis signaling axis, tumor necrosis factor-mediated signal transduction, nuclear factor kappa B signaling cascade, AGE-RAGE and African Trypanosomiasis (Figure 6).

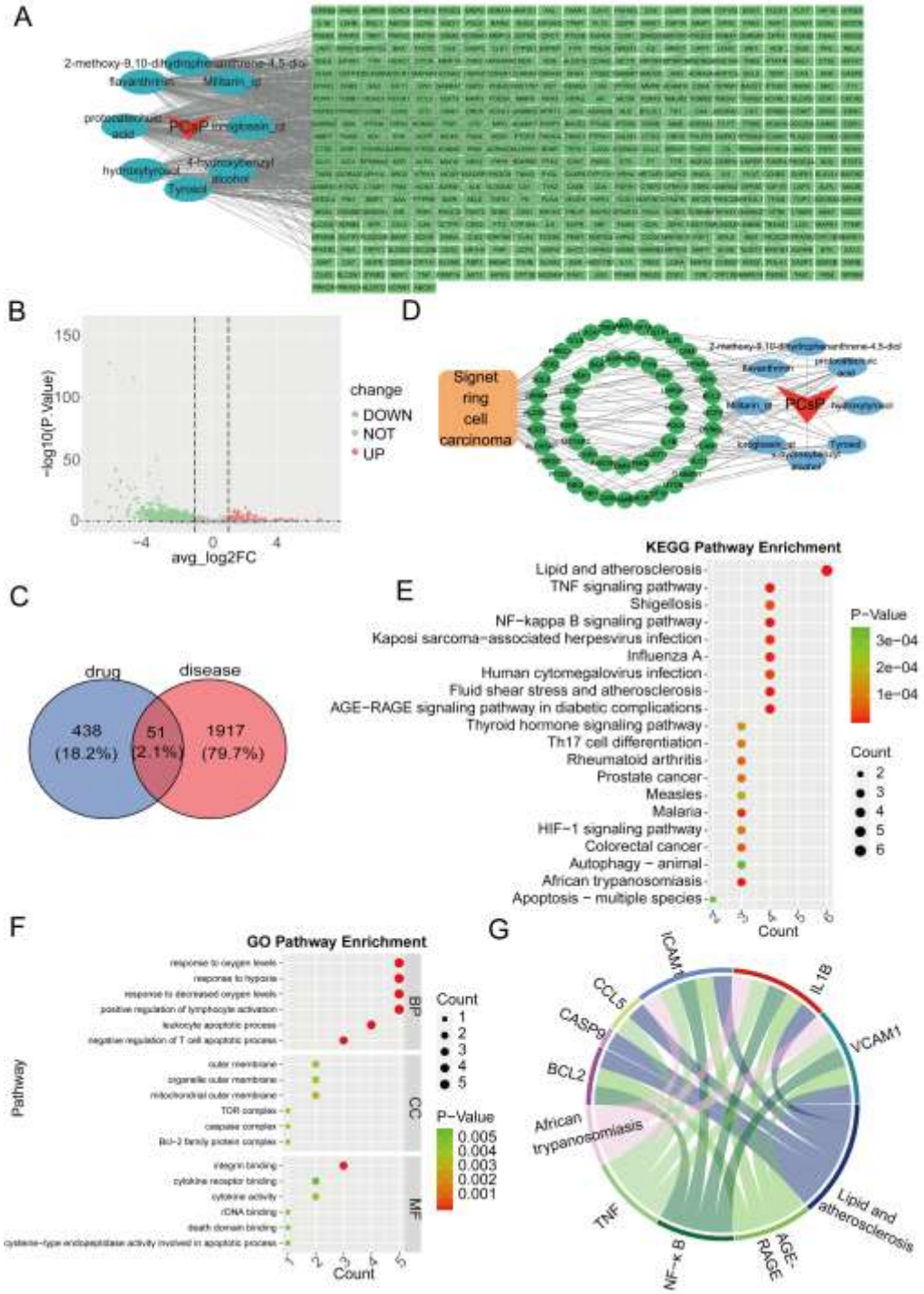

Figure 6 Identification of Macrophage-Related and PCsP Targets in gastric signet-Ring Cell Carcinoma and Comprehensive Anti-Tumor Pathway Analysis.

(A) The "Drug-Active Component-Target Gene" network; (B) Volcano plot of differential analysis between macrophage groups; (C) Venn diagram visualizing the common targets between drug targets and disease-lesioned cell-related targets; (D) The "Drug-Active Component-Intersecting Gene-Disease" network; (E) KEGG enrichment analysis results; (F) GO enrichment analysis results; (G) Chord diagram analysis of the key pathways involved in signal transduction.

3.6 Protein-Protein Interaction Network Analysis and Molecular Target Identification in PCsP-Mediated Response of Gastric Cancer-Lesioned Cells

A comprehensive PPI network analysis was conducted to elucidate the molecular interaction landscape underlying PCsP's therapeutic mechanisms in signet-ring cell carcinoma. The interaction network was generated via the

STRING database and visualized utilizing Cytoscape 3.8.2 software. Computational analyses performed through CytoHubba identified eight critical molecular targets: ICAM1, CASP9, MTOR, BCL2, VCAM1, IL-1β, CCL5, and HIF1A. Subsequent analyses demonstrated that PCsP's therapeutic efficacy is predominantly mediated through the modulation of HIF-1 and PI3K-Akt signal transduction pathways in GSRCC. An integrated pathway analysis was employed to delineate the complex molecular mechanisms governing PCsP's therapeutic activity. The investigation revealed hsa05417 as the primary PCsP-associated signaling pathway in signet-ring cell carcinoma. Multiple essential molecular mediators, including BCL2, IL-1β, ICAM1, VCAM1, and CASP9, exhibited significant involvement in these regulatory networks (Figure 7).

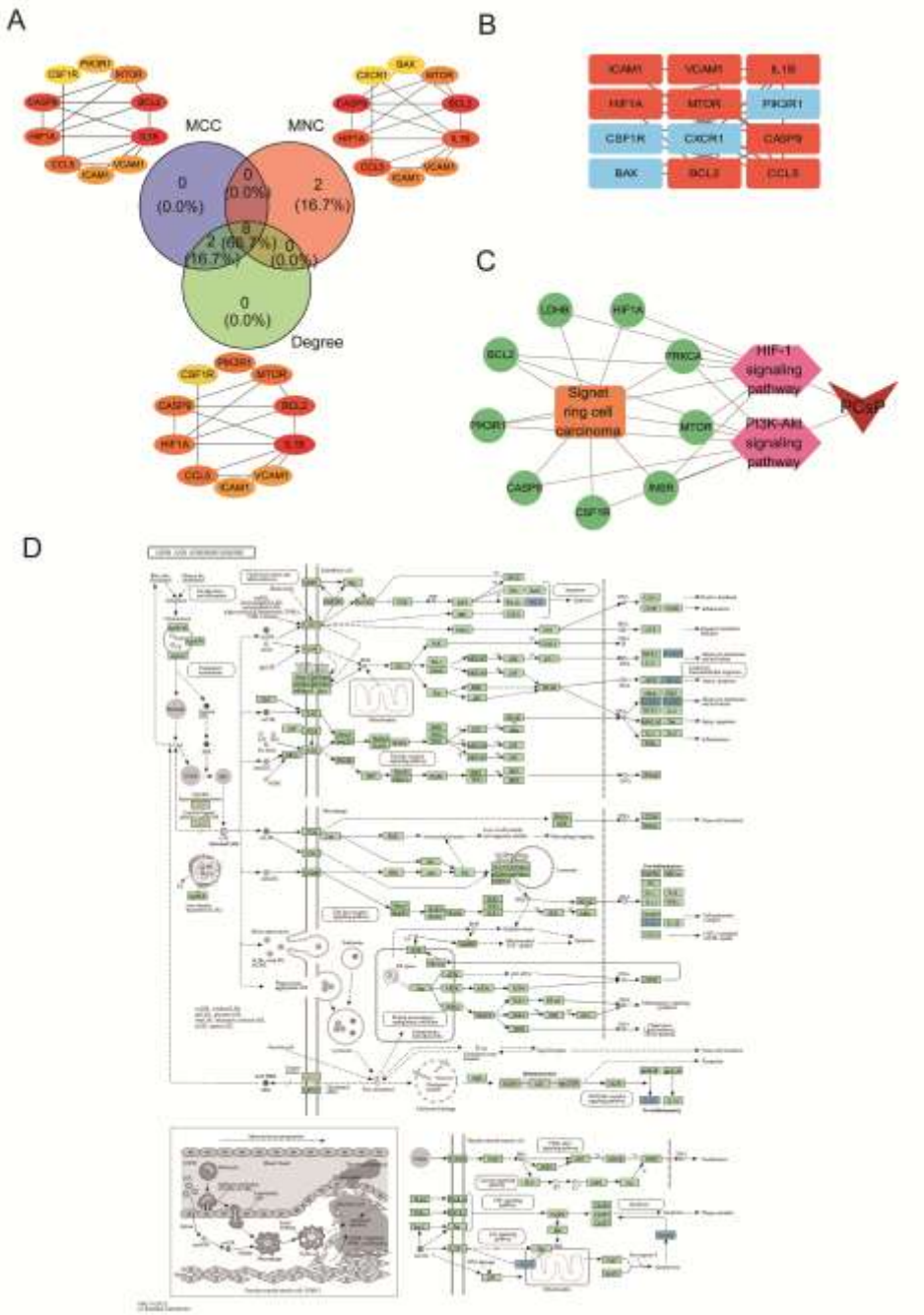

Figure 7 PPI Network Analysis and Central Target Screening of PCsP Against GSRCC-Lesioned Cells.

(A) Venn diagram visualizing the common targets between MCC, MNC and Degree targets; (B) Core target genes; (C) The "Drug-Pathway-Common Gene-Disease" network; (D) Lipid and atherosclerosis signaling pathway.

3.7 Molecular Docking Validation

To assess the molecular interactions, we performed computational docking analyses examining the binding characteristics between eight bioactive components identified in our study (2-methoxy-9,10-dihydrophenanthrene-4,5-diol, flavanthrinin-diol, flavanthrinin, hydroxytyrosol, loroglossin_qt, Militarin_qt, protocatechuic acid, Tyrosol, and 4-hydroxybenzyl alcohol) and their respective molecular targets (ICAM1, CASP9, MTOR, BCL2, VCAM1, IL-1β, CCL5, and HIF1A). The analysis employed specific binding affinity thresholds: interactions were considered present at values lower than -4.25 kcal·mol^{-1}, with significant binding indicated by affinities below -5.0 kcal·mol^{-1}, and strong interactions characterized by values under -7.0 kcal·mol^{-1}. Our docking simulations identified several noteworthy ligand-target interactions. The most significant binding affinities were observed in the following pairs: flavanthrinin-CASP9 complex (-8.90 kcal·mol^{-1}), 2-methoxy-9,10-dihydrophenanthrene-4,5-diol-CASP9 interaction (-8.80 kcal·mol^{-1}), loroglossin-CASP9 binding (-7.70 kcal·mol^{-1}), Militarin-CASP9 association (-7.60 kcal·mol^{-1}), and flavanthrinin-BCL2 complex (-7.20 kcal·mol^{-1}) (Figure 8).

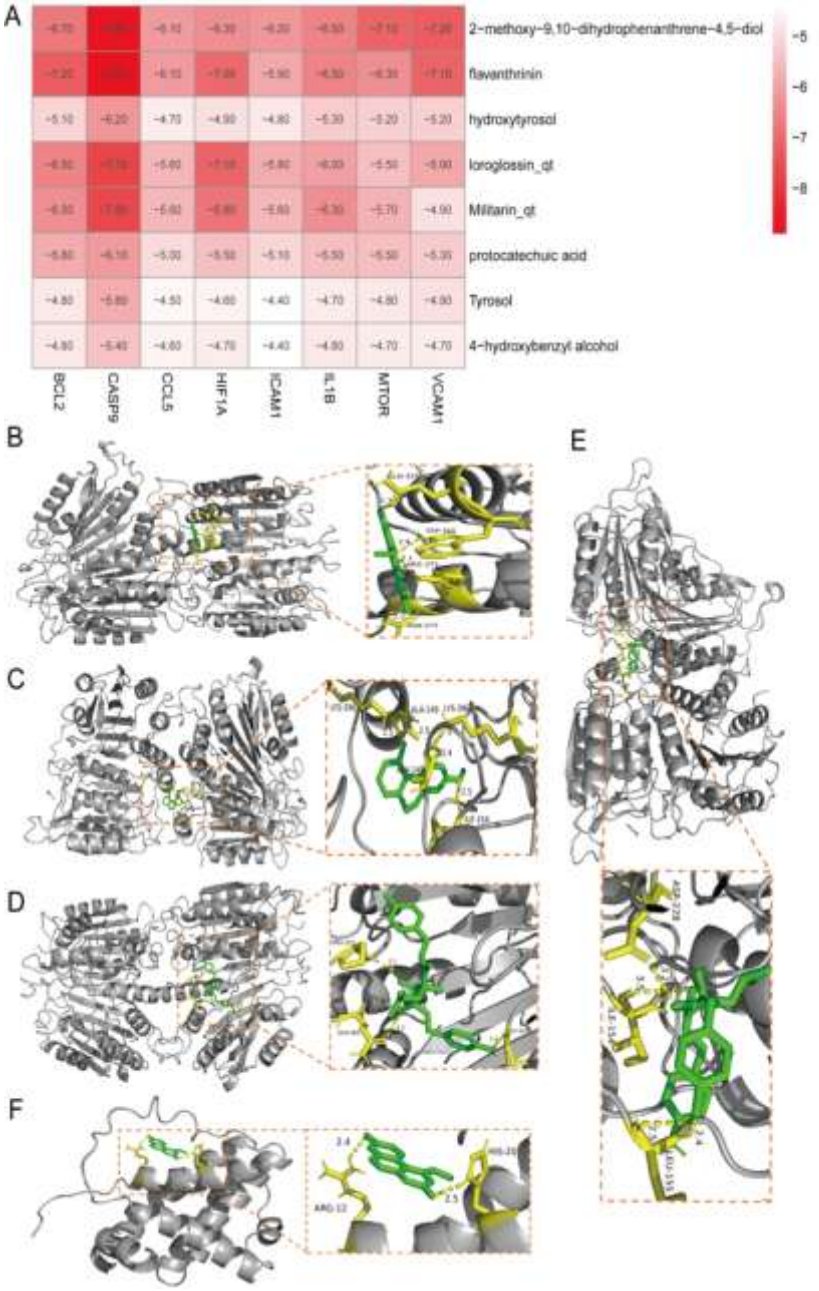

Figure 8 The results of molecular docking between the core targets and core ingredients (the five results with the lowest affinity).

(A) Heat map of molecular docking results; (B) Molecular docking results of flavanthrinin and CASP9 (afinity: -8.90); (C) Molecular docking results of 2-methoxy-9,10-dihydrophenanthrene-4,5-diol and CASP9 (affinity -8.80); (D) Molecular docking results of loroglossin and CASP9 (afinity: -7.70); (E) Molecular docking results of Militarin and CASP9 (afinity: -7.60); (F) Molecular docking results of flavanthrinin and BCL2 (afinity: -7.20).

4 Discussion

GSRCC represents a highly aggressive and therapeutically challenging subset of gastric neoplasms. Contemporary treatment protocols, encompassing radical surgical resection combined with systemic chemotherapeutic interventions, have failed to achieve satisfactory outcomes, with five-year survival rates remaining substantially inferior to other gastric malignancy subtypes. This pronounced therapeutic resistance primarily stems from SRCC's inherent chemoresistance mechanisms and its characteristic early metastatic dissemination[25]. Recent molecular and immunological investigations have revealed that GSRCC manifests a unique immunosuppressive tumor microenvironment, which significantly compromises host immune surveillance and contributes to adverse clinical trajectories[26]. Our research methodology integrated cutting-edge single-cell RNA sequencing (scRNA-seq) analytics with sophisticated network pharmacology to investigate the therapeutic potential and molecular mechanisms of PCsP in SRCC treatment. This multifaceted analytical framework enabled: (1) comprehensive immunological profiling of the SRCC microenvironment through scRNA-seq, elucidating cellular responses to PCsP intervention; (2) systematic identification of critical molecular targets and signal transduction pathways via network pharmacological analysis of PCsP's active components; and (3) computational validation of predicted molecular interactions through advanced molecular docking simulations, establishing a robust mechanistic framework for PCsP's therapeutic efficacy[27].

scRNA-seq methodology has transformed our understanding of cellular heterogeneity through comprehensive transcriptional profiling, yielding unprecedented insights into the TME, particularly regarding the diverse TAM subpopulations that orchestrate malignant progression[28]. TAMs merit intensive investigation due to their established correlation with adverse prognostic outcomes and their potential exploitation as therapeutic targets, especially in gastric carcinoma where they facilitate neoplastic proliferation and metastatic dissemination via multiple mechanistic pathways[29]. Analysis of the GSE163558 scRNA-seq dataset revealed distinct cellular constituents within the TME with marked heterogeneity observed within the macrophage compartment. Pseudotime trajectory analysis elucidated the developmental continuum of cellular states, identifying four discrete transcriptional modules associated with fundamental biological processes: chemotactic response mechanisms, cytoplasmic translation regulation, MHC protein complex assembly, and antiviral defense mechanisms. Cellular interaction analyses demonstrated that macrophages establish extensive reciprocal signaling networks with diverse cellular populations, predominantly through NAMPT-mediated pathways. Within the TME, macrophages exhibit heightened interconnectivity, establishing sophisticated communication networks that profoundly influence neoplastic evolution. Contemporary investigations have revealed that TAMs coordinate complex cellular interactions, notably through the PLTP+C1QC+ TAM subset, which modulates T lymphocyte function through elaborate cytokine and chemokine signaling cascades[30]. Recent experimental evidence has illuminated novel mechanisms through which endothelial cells contribute to tumor immunosuppression via their interactions with tumor-associated macrophages[31]. Specifically, tumor-associated endothelial cells elaborate interleukin-6 which, in concert with CSF-1, induces HIF-2α-dependent arginase-1 expression via PPAR-γ signaling, thereby promoting alternative macrophage polarization and facilitating glioblastoma multiforme progression[32].

Contemporary research methodologies will utilize network pharmacology to investigate the intricate pathogenic mechanisms and potential therapeutic interventions targeting macrophage functionality. This sophisticated analytical framework integrates diverse biological systems, pharmacological agents, and disease states through a

comprehensive network-based approach, exhibiting notable concordance with the integrative principles of TCM[33]. The analytical power of this approach in forecasting secondary pharmacological effects through its multifaceted disease-drug-target paradigm has positioned it as an essential methodology in modern TCM investigation[34, 35]. Clinical investigations have revealed that traditional Chinese pharmaceutical preparations effectively regulate neoplastic progression and dissemination via immunological modulation [36] .

Our investigation into PCsP's molecular mechanism of action in gastric cancer employed a network pharmacology approach. Through systematic analysis incorporating ADME criteria, we successfully identified eight bioactive constituents and their corresponding 489 molecular targets via comprehensive screening of TCMSP and TCMID databases. Parallel analysis of GEO datasets yielded 1,968 gastric cancer-related genetic targets. Subsequent intersection analysis through Venn diagramming revealed 51 shared molecular targets between PCsP-associated pathways and gastric cancer-related molecular networks.

Our investigation into PCsP's therapeutic mechanisms in gastric cancer employed both GO and KEGG pathway analyses. The GO analysis identified enriched target genes primarily involved in oxygen-related biological processes, including responses to varying oxygen levels, hypoxia adaptation, and regulation of lymphocyte activation pathways. The KEGG pathway investigation revealed that PCsP exerts its anti-gastric cancer effects via diverse molecular pathways, notably those involving lipid metabolism and atherosclerosis, TNF signaling networks, and the NF-κB cascade. Particularly noteworthy was the pronounced enrichment of both TNF and NF-κB pathways, indicating their crucial mechanistic roles in PCsP's therapeutic efficacy against gastric cancer. The inflammatory mediator TNF-α, characterized by its multiple biological functions, significantly impacts tumor development by regulating immune responses and blood vessel formation[37]. Studies indicate that H. pylori infection elevates TNF-α levels, facilitating the emergence of premalignant gastric conditions - specifically intestinal metaplasia and cellular dysplasia - which may progress toward malignancy[38]. The effects of TNF-α' are primarily orchestrated via two major signaling pathways: NF-κB and MAPK cascades. Current evidence suggests that activation of the NF-κB pathway upregulates PD-L1 expression in mast cells, resulting in suppressed T-cell responses and accelerated gastric cancer progression[39] . Within the tumor microenvironment, both infiltrating macrophages and malignant gastric cells demonstrate NF-κB-regulated expression of VEGF and VEGF-C, thereby promoting both blood and lymphatic vessel development[40]. Contemporary targeted therapeutic approaches, particularly HER-2 antagonists and PI3K/AKT pathway inhibitors, achieve their pro-apoptotic effects through downstream suppression of NF-κB activity[41, 42]. Protocatechuic acid, isolated from PCsP, demonstrates therapeutic efficacy through concurrent molecular mechanisms: regulation of the BCL2/NF-κB signaling axis and modulation of CCL5-mediated TNF pathway activity. These mechanistic interactions facilitate anti-inflammatory responses, immune system modulation, favorable gastric cancer outcomes, and enhanced patient survival metrics. Additional mechanistic studies are essential to fully characterize the molecular pathways underlying these observed therapeutic benefits.

Molecular docking analyses were employed to investigate the mechanistic underpinnings of PCsP's therapeutic potential in GC. The investigation focused on eight key target proteins-BCL2, CASP9, CCL5, HIF1A, ICAM1, IL1B, MTOR, and VCAM1—alongside their corresponding bioactive constituents sourced from TCMSP, including 2-methoxy-9,10-dihydrophenanthrene-4,5-diol, flavanthrinin, hydroxytyrosol, loroglossin_qt, Militarin_qt, protocatechuic acid, Tyrosol, and 4-hydroxybenzyl alcohol. In molecular docking studies, the strength of receptor-ligand interactions is inversely proportional to binding energy values. Contemporary research standards consider binding energies below -5 kcal/mol as a reliable indicator of favorable molecular interactions[43-45]. The computational investigation demonstrated that the bioactive components of PCsP exhibited strong molecular interactions with CASP9 and BCL2 proteins, with docking energies consistently falling below the -5 kcal/mol threshold. These computational outcomes align with the protein-protein interaction analyses,

reinforcing the potential significance of these proteins as therapeutic targets. The observed molecular associations were facilitated primarily through hydrogen bonds and hydrophobic forces, offering insights into the possible mechanisms by which PCsP's components achieve their anti-cancer effects in gastric malignancies.

5 Limitations

This study acknowledges certain constraints in its methodology. The reliability of our predictions depends largely on the accuracy of bioactive compound data and target information obtained from published literature and established databases. Additional research incorporating LC/MS analytical techniques for active compound identification, combined with comprehensive metabolomic and pharmacokinetic evaluations, would strengthen these findings. Furthermore, while our computational approach provides valuable insights, definitive confirmation requires rigorous clinical trials and animal model studies.

6 Conclusion

GSRCC, a distinct phenotypic variant of gastric cancer, exhibits a pronounced propensity for peritoneal dissemination. While PCsP demonstrates anticancer efficacy through multiple mechanisms, including proliferation suppression, apoptosis induction, and metastatic cascade inhibition, its molecular targets and underlying biological processes in GSRCC remain incompletely elucidated. This investigation employed single-cell RNA seq to delineate the immunological landscape within tumor tissues, specifically analyzing the distribution patterns of eight immune cell populations. Furthermore, dimensional reduction clustering analysis of the macrophage subset was conducted to elucidate cellular trajectory patterns, transcriptional regulatory networks, and intercellular communication mechanisms.

Network pharmacology methodologies were utilized to elucidate the therapeutic mechanisms of PCSP in GSRCC treatment. The analysis identified eight bioactive constituents and 489 putative PCSP targets, with 51 targets showing overlap between PCSP and gastric cancer pathways. Topological network analysis revealed eight pivotal molecular targets among these intersecting elements. Gene Ontology enrichment analysis demonstrated that PCSP's anti-gastric cancer activity encompasses diverse biological processes. Pathway analysis through the Kyoto Encyclopedia of KEGG revealed that PCsP's therapeutic effects are predominantly mediated through the lipid and atherosclerosis signaling cascade. Molecular docking analyses confirmed substantial binding affinities between the identified bioactive compounds and their respective molecular targets.

This comprehensive investigation has successfully characterized the bioactive constituents, molecular targets, and signaling pathways through which PCsP exerts its therapeutic effects in gastric cancer, thereby establishing a foundation for subsequent mechanistic investigations. Moreover, the identified bioactive compounds represent promising candidates for therapeutic development in gastric cancer treatment.

Acknowledgments

The authors extend their profound gratitude to the participants for their invaluable contributions to this study.

Conflict of interest Statement:

The authors declare that the research has no competing interests.

Funding Statement:

This work was supported by the Dongguan Science and Technology of Social Development Program under Grant NO.20221800906122.

Reference

1. Sung H, Ferlay J, Siegel RL, et al. Global Cancer Statistics 2020: GLOBOCAN Estimates of Incidence and Mortality Worldwide for 36 Cancers in 185 Countries. CA Cancer J Clin. 2021; 71: 209-49.
2. Lopez MJ, Carbajal J, Alfaro AL, et al. Characteristics of gastric cancer around the world. Crit Rev Oncol Hematol. 2023; 181: 103841.
3. Guan W-L, He Y and Xu R-H. Gastric cancer treatment: recent progress and future perspectives. J Hematol Oncol. 2023; 16: 57.
4. Zhao W, Jia Y, Sun G, et al. Single-cell analysis of gastric signet ring cell carcinoma reveals cytological and immune microenvironment features. Nat Commun. 20 23; 14: 2985.
5. Cavalcanti E, Armentano R and Lolli I.

Crohn's Disease Following Rituximab Treatment for Follicular Lymphoma in a Patient with Synchronous Gastric Signet Ring Cells Carcinoma: A Case Report and Literature Review. Cancer Res Treat. 2020; 52: 1291-5.
6. Ding N, Liu Q, Du J, et al. Individualised adjuvant immunotherapy with neoantigen-reactive T cells for gastric signet-ring cell carcinoma. Clin Transl Immunology. 2023; 12: e1467.
7. Tan Z. Recent Advances in the Surgical Treatment of Advanced Gastric Cancer: A Review. Med Sci Monit. 2019; 25: 3537-41.
8. Chen J, Liu K, Luo Y, et al. Single-Cell Profiling of Tumor Immune Microenvironment Reveals Immune Irresponsiveness in Gastric Signet-Ring Cell Carcinoma. Gastroenterology. 2023; 165: 88-103.
9. Smyth EC, Nilsson M, Grabsch HI, van Grieken NC and Lordick F. Gastric cancer. Lancet. 2020; 396: 635-48.
10. Li Y, Zhu Z, Ma F, Xue L and Tian Y. Gastric Signet Ring Cell Carcinoma: Current Management and Future Challenges. Cancer Manag Res. 2020; 12: 7973-81.
11. Li Y, Zhong Y, Xu Q, Zhu Z and Tian Y. Prognostic Significance of Signet Ring Cells in Gastric Cancer: The Higher Proportion, The Better Survival. Front Oncol. 2021; 11: 713587.
12. Dai Z, Tan C, Wang J, et al. Traditional Chinese medicine for gastric cancer: An evidence mapping. Phytother Res. 2024; 38: 2707-23.
13. Jiang Y, Wang Y, Chen G, et al. Nicotinamide metabolism face-off between macrophages and fibroblasts manipulates the microenvironment in gastric cancer. Cell Metab. 2024; 36: 1806-22.e11.
14. Sun Z, Zhang T, Ahmad MU, et al. Comprehensive assessment of immune context and immunotherapy response via noninvasive imaging in gastric cancer. J Clin Invest. 2024; 134.
15. Zhao S, Liu Y, Ding L, et al. Gastric cancer immune microenvironment score predicts neoadjuvant chemotherapy efficacy and prognosis. J Pathol Clin Res. 2024; 10: e12 378.
16. Zeng D, Li M, Zhou R, et al. Tumor Microenvironment Characterization in Gastric Cancer Identifies Prognostic and Immunotherapeutically Relevant Gene Signatures. Cancer Immunol Res. 2019; 7: 73 7-50.
17. Jiang Y, Xie J, Huang W, et al. Tumor Immune Microenvironment and Chemosensitivity Signature for Predicting Response to Chemotherapy in Gastric Cancer. Cancer Immunol Res. 2019; 7: 2065-73.
18. Qiu S, Xie L, Lu C, et al. Gastric cancer-derived exosomal miR-519a-3p promotes liver metastasis by inducing intrahepatic M2-like macrophage-mediated angiogenesis. J Exp Clin Cancer Res. 2022; 41: 296.
19. Lin Y, Jing X, Chen Z, et al. Histone deacetylase-mediated tumor microenvironment characteristics and synergistic immunotherapy in gastric cancer. Theranostics. 2023; 13: 4574-600.
20. Li Y, Hu X, Lin R, et al. Single-cell landscape reveals active cell subtypes and their interaction in the tumor microenvironment of gastric cancer. Theranostics. 2022; 12: 3818-33.
21. Zheng H, Wang G, Liu M and Cheng H. Traditional Chinese medicine inhibits PD-1/PD-L1 axis to sensitize cancer immunotherapy: a literature review. Front Oncol. 2023; 13: 1168226.
22. Zhu J, Liu Z, Pu Y, Xu J, Zhang S and Bao Y. Green synthesized gold nanoparticles from Pseudobulbus Cremastrae seu Pleiones show efficacy against hepatic carcinoma potentially through immunoregulation. Drug Deliv. 2022; 29: 1983-93.
23. Zhou C, Jia Y, Zhang Q, et al. A systematic study of Pseudobulbus Cremastrae seu Pleiones: Characteristics, Origin, chemical composition and toxicology. J Ethnopharmacol. 2025; 337: 118923.
24. Jiang H, Yu D, Yang P, et al. Revealing the transcriptional heterogeneity of organ-specific metastasis in human gastric cancer using single-cell RNA Sequencing. Clin Transl Med. 2022; 12: e730.
25. Gertsen EC, van der Veen A, Brenkman HJF, et al. Multimodal Therapy Versus Primary Surgery for Gastric and Gastroesophageal Junction Diffuse Type Carcinoma, with a Focus on Signet Ring Cell Carcinoma: A Nationwide Study. Ann Surg Oncol. 2024; 31:

1760-72.
26. Liu X, Xu D, Huang C, et al. Regulatory T cells and M2 macrophages present diverse prognostic value in gastric cancer patients with different clinicopathologic characteristics and chemotherapy strategies. J Transl Med. 2019; 17: 192.
27. Zhai Y, Zhang J, Huang Z, et al. Single-cell RNA sequencing integrated with bulk RNA sequencing analysis reveals diagnostic and prognostic signatures and immunoinfiltration in gastric cancer. Comput Biol Med. 2023; 163: 107239.
28. Wu SZ, Al-Eryani G, Roden DL, et al. A single-cell and spatially resolved atlas of human breast cancers. Nat Genet. 2021; 53: 1334-47.
29. Ji L, Fu G, Huang M, et al. scRNA-seq of colorectal cancer shows regional immune atlas with the function of CD20(+) B cells. Cancer Lett. 2024; 584: 216664.
30. Hong F, Meng Q, Zhang W, et al. Single-Cell Analysis of the Pan-Cancer Immune Microenvironment and scTIME Portal. Cancer Immunol Res. 2021; 9: 939-51.
31. Do MH, Shi W, Ji L, et al. Reprogramming tumor-associated macrophages to outcompete endovascular endothelial progenitor cells and suppress tumor neoangiogenesis. Immunity. 2023; 56: 2555-69.e5.
32. Yang F, Akhtar MN, Zhang D, et al. An immunosuppressive vascular niche drives macrophage polarization and immunotherapy resistance in glioblastoma. Sci Adv. 2024; 10: eadj4678.
33. Duan Z-L, Wang Y-J, Lu Z-H, et al. Wumei Wan attenuates angiogenesis and inflammation by modulating RAGE signaling pathway in IBD: Network pharmacology analysis and experimental evidence. Phytomedicine. 2023; 111: 154658.
34. Zhang G-B, Li Q-Y, Chen Q-L and Su S-B. Network pharmacology: a new approach for chinese herbal medicine research. Evid Based Complement Alternat Med. 2013; 2013: 621423.
35. Wang X, Wang Z-Y, Zheng J-H and Li S. TCM network pharmacology: A new trend towards combining computational, experimental and clinical approaches. Chin J Nat Med. 2021; 19: 1-11.
36. Loo WTY, Jin LJ, Chow LWC, Cheung MNB and Wang M. Rhodiola algida improves chemotherapy-induced oral mucositis in breast cancer patients. Expert Opin Investig Drugs. 2010; 19 Suppl 1: S91-100.
37. Lv Y, Zhao Y, Wang X, et al. Increased intratumoral mast cells foster immune suppression and gastric cancer progression through TNF-alpha-PD-L1 pathway. J Immunother Cancer. 2019; 7: 54.
38. Kuzuhara T, Suganuma M, Oka K and Fujiki H. DNA-binding activity of TNF-alpha inducing protein from Helicobacter pylori. Biochem Biophys Res Commun. 2007; 362: 805-10.
39. Wang Y, Liu J and Wang Y. Role of TNF-alpha-induced m6A RNA methylation in diseases: a comprehensive review. Front Cell Dev Biol. 2023; 11: 1166308.
40. Sokolova O and Naumann M. NF-kappaB Signaling in Gastric Cancer. Toxins (Basel). 2017; 9.
41. Zhou X-X, Ji F, Zhao J-L, Cheng L-F and Xu C-F. Anti-cancer activity of anti-p185HER-2 ricin A chain immunotoxin on gastric cancer cells. J Gastroenterol Hepatol. 2010; 25: 1266-75.
42. Shin J-Y, Kim J-O, Lee SK, Chae H-S and Kang J-H. LY294002 may overcome 5-FU resistance via down-regulation of activated p-AKT in Epstein-Barr virus-positive gastric cancer cells. BMC Cancer. 2010; 10: 425.
43. Zhang W, Tian W, Wang Y, et al. Explore the mechanism and substance basis of Mahuang FuziXixin Decoction for the treatment of lung cancer based on network pharmacology and molecular docking. Comput Biol Med. 2022; 151: 106293.
44. Li X, Wei S, Niu S, et al. Network pharmacology prediction and molecular docking-based strategy to explore the potential mechanism of Huanglian Jiedu Decoction against sepsis. Comput Biol Med. 2022; 144: 105389.
45. Dai Z, Zhang J, Xu W, Du P, Wang Z and Liu Y. Single-Cell Sequencing-Based Validation of T Cell-Associated Diagnostic Model Genes and Drug Response in Crohn's Disease. Int J Mol Sci. 2023; 24.